

# Probing New Physics in $B \rightarrow K^{(*)}\ell^+\ell^-$ decays

Chuan-Hung Chen<sup>a</sup> and C. Q. Geng<sup>b,c</sup>

<sup>a</sup> *Institute of Physics, Academia Sinica  
Taipei, Taiwan 115, Republic of China*

<sup>b</sup> *Department of Physics, National Tsing Hua University  
Hsinchu, Taiwan 300, Republic of China*

<sup>c</sup> *Theory Group, TRIUMF  
4004 Wesbrook Mall, Vancouver, B.C. V6T 2A3, Canada*

## Abstract

We study the exclusive decays of  $B \rightarrow K^{(*)}\ell^+\ell^-$  by the results in the perturbative QCD with the heavy quark effective theory and lattice calculations. We obtain the form factors for the  $B \rightarrow K^{(*)}$  transitions in the whole allowed region. Our predictions on the branching ratios of  $B \rightarrow K\ell^+\ell^-$ ,  $B \rightarrow K^*e^+e^-$ , and  $B \rightarrow K^*\mu^+\mu^-$  are  $0.53 \pm 0.05_{-0.07}^{+0.10}$ ,  $1.68 \pm 0.17_{-0.09}^{+0.14}$ , and  $1.34 \pm 0.13_{-0.06}^{+0.11} \times 10^{-6}$ , where the errors are from the quark mixing elements and hadronic effects, respectively. We also find that our definitions of the T-odd observable and the up-down asymmetry of the  $K$  meson in  $B \rightarrow K^*\ell^+\ell^- \rightarrow K\pi\ell^+\ell^-$  can be used to probe new physics.

# 1 Introduction

The flavor-changing neutral current (FCNC) processes of  $B \rightarrow K^{(*)}\ell^+\ell^-$  ( $\ell = e, \mu, \tau$ ) are suppressed and induced by electroweak penguin and box diagrams in the standard model (SM) with branching ratios of  $\mathcal{O}(10^{-7} - 10^{-6})$  [1, 2, 3, 4]. Recently, the decay modes of  $B \rightarrow K\ell^+\ell^-$  ( $\ell = e, \mu$ ) have been observed with  $Br(B \rightarrow K\ell^+\ell^-) = (0.75_{-0.21}^{+0.25} \pm 0.09) \times 10^{-6}$  [5] and  $(0.78_{-0.20}^{+0.24+0.11}) \times 10^{-6}$  [6, 7], at the Belle detector in the KEKB  $e^+e^-$  storage ring and the BABAR detector in the PEP-II B factory by using  $29.1 fb^{-1}$  and  $77.8 fb^{-1}$  data samples, respectively. Experimental searches at the B-factories for  $B \rightarrow K^*\ell^+\ell^-$  are also close to the theoretical predicted ranges [5, 6, 7]. At BABAR, an excess of events over background with estimated significance of  $2.8\sigma$  has been observed and  $Br(B \rightarrow K^*\ell^+\ell^-) = (1.68_{-0.58}^{+0.68} \pm 0.28) \times 10^{-6}$  has been obtained [7]. It is clear that these FCNC rare decays are important for not only testing the SM but probing new physics such as supersymmetric heavy particles in SUSY models, appearing virtually in the loop diagrams to interfere with those in the SM.

It is known that one of the main theoretical uncertainties in studying exclusive hadron decays arises from the calculations of matrix elements. In our previous work [4], we calculated the relevant transition form factors for  $B \rightarrow K(K^*)$  decays in the perturbative QCD (PQCD) approach with the phenomenological wave functions, which are chosen by fitting with the experimental measurements of  $B \rightarrow K\pi$  and  $B \rightarrow K^*\gamma$  decays. Moreover, in order to compensate the increasing soft gluon effects in the slow recoil region, we used trial  $q^2$ -dependent wave functions instead of unknown  $b$ -dependent wave functions, where  $b$  is the conjugate variable of transverse momentum of valence quark. However, with the trial wave functions, it is difficult to estimate the errors in the  $B \rightarrow K(K^*)$  form factors as well as the branching ratios and other physical observables in  $B \rightarrow K(K^*)\ell^+\ell^-$  decays.

To get a control of theoretical uncertainties in  $B \rightarrow K(K^*)\ell^+\ell^-$  decays, in this paper, we first recalculate the corresponding form factors at the large recoil region of the momentum transfer  $q^2 \rightarrow 0$  with the improved PQCD approach that includes not only  $k_T$  resummation, for removing end-point singularities, but also threshold resummation, for smearing the double logarithmic divergence arising from weak corrections [8]. The involved wave functions are used up to twist-3, derived from QCD sum rule [9]. Then, we fit these results with those from the heavy quark effective theory (HQET) and the lattice QCD (LQCD) calculations in

the large  $q^2$  region to get the whole  $q^2$  allowed values.

To emphasize the role of new physics, we define some P and T-odd observables. We will show that the effects of some observables are small in the SM but can be large and measurable in models with new physics.

The paper is organized as follows. In Sec. II, we present the form factors of the  $B \rightarrow K^{(*)}$  transitions in the framework of the PQCD. In Sec. III, we estimate the decay rates of  $B \rightarrow K^{(*)}\ell^+\ell^-$  in the SM. We also study the polarization of  $K^*$  in  $B \rightarrow K^*\ell^+\ell^-$ . In Sec. IV, we discuss P and T violating effects in  $B \rightarrow K^*\ell^+\ell^- \rightarrow K\pi\ell^+\ell^-$ . We present our conclusions in Sec. V.

## 2 form factors in $B \rightarrow K^{(*)}$ transition

To obtain the transition elements of  $B \rightarrow H$  ( $H = K, K^*$ ) with various weak vertices, we parametrize them in terms of the relevant form factors as follows:<sup>a</sup>

$$\begin{aligned}
\langle K(p_2, \epsilon) | V_\mu | \bar{B}(p_1) \rangle &= f_+(q^2) \left\{ P_\mu - \frac{P \cdot q}{q^2} \right\} + \frac{P \cdot q}{q^2} f_0(q^2) q_\mu, \\
\langle K(p_2, \epsilon) | T_{\mu\nu} q^\nu | \bar{B}(p_1) \rangle &= \frac{f_T(q^2)}{m_B + m_K} \left\{ P \cdot q q_\mu - q^2 P_\mu \right\}, \\
\langle K^*(p_2, \epsilon) | V_\mu | \bar{B}(p_1) \rangle &= i \frac{V(q^2)}{m_B + m_{K^*}} \varepsilon_{\mu\alpha\beta\rho} \epsilon^{*\alpha} P^\beta q^\rho, \\
\langle K^*(p_2, \epsilon) | A_\mu | \bar{B}(p_1) \rangle &= 2m_{K^*} A_0(q^2) \frac{\epsilon^* \cdot q}{q^2} q_\mu + (m_B + m_{K^*}) A_1(q^2) \left( \epsilon_\mu^* - \frac{\epsilon^* \cdot q}{q^2} q_\mu \right) \\
&\quad - A_2(q^2) \frac{\epsilon^* \cdot q}{m_B + m_{K^*}} \left( P_\mu - \frac{P \cdot q}{q^2} q_\mu \right), \\
\langle K^*(p_2, \epsilon) | T_{\mu\nu} q^\nu | \bar{B}(p_1) \rangle &= -iT_1(q^2) \varepsilon_{\mu\alpha\beta\rho} \epsilon^{*\alpha} P^\beta q^\rho, \\
\langle K^*(p_2, \epsilon) | T_{\mu\nu}^5 q^\nu | \bar{B}(p_1) \rangle &= T_2(q^2) \left( \epsilon_\mu^* P \cdot q - \epsilon^* \cdot q P_\mu \right) + T_3(q^2) \epsilon^* \cdot q \left( q_\mu - \frac{q^2}{P \cdot q} P_\mu \right) \quad (1)
\end{aligned}$$

where  $V_\mu = \bar{s}\gamma_\mu b$ ,  $A_\mu = \bar{s}\gamma_\mu\gamma_5 b$ ,  $T_{\mu\nu} = \bar{s}i\sigma_{\mu\nu}b$ , and  $T_{\mu\nu}^5 = \bar{s}i\sigma_{\mu\nu}\gamma_5 b$ . To evaluate the  $q^2$ -dependent form factors in Eq. (1), we use two QCD methods. One is for the large recoil region of small  $q^2$  and the other for the zero recoil region of high  $q^2$ .

It is known that in the large energy transfer processes, the hadronic transition matrix elements can be calculated by the Lepage-Brodsky (LB) [10] formalism. However, the original LB formalism suffers logarithmic and linear singularities in twist-2 and twist-3 wave functions from the end-point region with a momentum fraction  $x \rightarrow 0$ , respectively. In order to

---

<sup>a</sup>The relationships between various definitions of the form factors have been given in Appendix of Ref. [4].

handle these singularities, the strategy of introducing the  $k_T$  resummation and threshold resummation has been proposed. It has been shown that due to the induced Sudakov factors which make the  $|k_T|$  from  $\bar{\Lambda}$  scale to  $(\bar{\Lambda}m_B)^{1/2}$  with  $\bar{\Lambda} = m_B - m_b$  [8] and  $m_b$  being the  $b$ -quark mass, the singularities do not exist in a self-consistent improved PQCD analysis [11]. Furthermore, due to the different properties of wave functions at end-point region, it is found that the power behaviors in  $B \rightarrow K(K^*)$  form factors are the same in twist-2 and 3 wave functions [12]. It shows the importance of twist-3 contributions. According to Ref. [12], we also know that other higher twist wave functions exist extra power suppression in  $m_0/m_B$  with  $m_0$  being the chiral symmetry breaking parameter so that they are neglected in our considerations.

Recently, the applications of the PQCD approach to exclusive heavy  $B$  meson decays, such as  $B \rightarrow K\pi$  [13],  $B \rightarrow \pi\pi(KK)$  [14, 15],  $B \rightarrow \phi\pi(K)$  [16, 17], and  $B \rightarrow \rho K$  [18] decays, have been studied and found that all of them are consistent with the current experimental data. As known, in these two-body charmless decays, the squared momentum transfer is around  $m_M^2$  with  $M$  being a pseudoscalar or a vector meson. That is, the PQCD can work well at the region of  $q^2 \simeq m_M^2$ . Therefore, we will apply the predicted results of the PQCD to the large recoil region where the final outgoing meson  $M$  carries a large energy and momentum. As to the opposite region near  $q^2|_{max}$ , we can use the relations among the form factor given in the HQET [19] by substituting the calculated values of the form factors from the LQCD [20] in them to get the remaining ones. Once the values of the form factors at both end edges of the allowed  $q^2$  are determined, we can find the  $q^2$ -dependent ones by fitting the forms

$$F_i(q^2) = \frac{F_i(0)}{1 + \sigma_1 s + \sigma_2 s^2} \quad (2)$$

where  $s = q^2/m_B^2$ ,  $F_i(0)$  are form factors at  $q^2 = 0$ , and  $\sigma_{1,2}$  are the fitted parameters.

We now show how to obtain the form factors at large and zero recoil:

## 2.1 At large recoil

In  $B \rightarrow H\ell^+\ell^-$  ( $H = K, K^*$ ) decays, the  $B$  meson momentum  $p_1$ ,  $H$  meson momentum  $p_2$  and  $K^*$  polarization vector  $\epsilon$  in the  $B$  meson rest frame and light-cone coordinate are taken to be

$$p_1 = \frac{m_B}{\sqrt{2}}(1, 1, \vec{0}_\perp), \quad p_2 = \frac{m_B}{\sqrt{2}\eta}(\eta^2, r_H^2, \vec{0}_\perp),$$

$$\epsilon_L = \frac{1}{\sqrt{2}r_{K^*}\eta}(\eta^2, -r_{K^*}^2, \vec{0}_\perp), \quad \epsilon_T(\pm) = \frac{1}{\sqrt{2}}(0, 0, 1, \pm i) \quad (3)$$

where  $\eta \simeq 1 - s$  and  $r_H = m_H/m_B$ , while those for the spectators of B and H sides are expressed as

$$k_1 = \left(0, x_1 \frac{m_B}{\sqrt{2}}, \vec{k}_{1\perp}\right), \quad k_2 = \left(x_2 \frac{m_B}{\sqrt{2}}\eta, 0, \vec{k}_{2\perp}\right), \quad (4)$$

respectively. In our calculations, we will neglect the small contributions from  $m_{u,d,s}$  and  $\bar{\Lambda}$  as well as  $m_H^2$  due to the on-shell condition of the valence-quark preserved. From the results of Ref. [9], the  $K^{(*)}$  meson distribution amplitudes can be derived up to twist-3 as follows:

$$\begin{aligned} \langle K(p) | \bar{s}(z)_j d(0)_l | 0 \rangle &= -\frac{i}{\sqrt{2N_c}} \int_0^1 dx e^{ixp \cdot z} \{ \not{p} \gamma_5 \phi_K(x) + m_K^0 [\gamma_5]_{lj} \phi_K^p(x) \\ &\quad + m_K^0 [\gamma_5 (\not{n}_+ \not{n}_- - 1)]_{lj} \phi_K^t(x) \}, \\ \langle K^*(p, \epsilon_L) | \bar{s}(z)_j d(0)_l | 0 \rangle &= \frac{1}{\sqrt{2N_c}} \int_0^1 dx e^{ixp \cdot z} \{ m_{K^*} [\epsilon_L]_{lj} \phi_{K^*}(x) + [\epsilon_L \not{p}]_{lj} \phi_{K^*}^t(x) \\ &\quad + m_{K^*} [I]_{lj} \phi_{K^*}^s(x) \}, \\ \langle K^*(p, \epsilon_T) | \bar{s}(z)_j d(0)_l | 0 \rangle &= \frac{1}{\sqrt{2N_c}} \int_0^1 dx e^{ixp \cdot z} \{ m_{K^*} [\epsilon_T]_{lj} \phi_{K^*}^v(x) + [\epsilon_T \not{p}]_{lj} \phi_{K^*}^T(x) \\ &\quad + \frac{m_{K^*}}{p \cdot n_-} i \epsilon_{\mu\nu\rho\sigma} [\gamma_5 \gamma^\mu]_{lj} \epsilon_T^\nu p^\rho n_-^\sigma \phi_{K^*}^a(x) \}, \end{aligned} \quad (5)$$

where  $n_+ = (1, 0, \vec{0}_\perp)$  and  $n_- = (0, 1, \vec{0}_\perp)$ . In Eq. (5),  $\phi_K(x)$ ,  $\phi_{K^*}(x)$  and  $\phi_{K^*}^T(x)$  are the twist-2 wave functions, and all the remaining ones belong to the twist-3. Their explicit expressions can be found in Ref. [9].

By using the LB formalism with including  $k_T$  and threshold resummation, the form factors  $f_+(q^2)$ ,  $f_-(q^2)$ , and  $f_T(q^2)$  in  $B \rightarrow K$  can be written as

$$\begin{aligned} f_+(q^2) &= f_1(q^2) + f_2(q^2), \\ f_0(q^2) &= f_1(q^2) \left(1 + \frac{q^2}{m_B^2}\right) + f_2(q^2) \left(1 - \frac{q^2}{m_B^2}\right), \end{aligned} \quad (6)$$

where

$$\begin{aligned} f_1(q^2) &= 8\pi C_F m_B^2 r_K \int_0^1 [dx] \int_0^\infty b_1 db_1 b_2 db_2 \phi_B(x_1, b_1) [\phi_K^p(x_2) - \phi_K^t(x_2)] \\ &\quad \times E(t^{(1)}) h^K(x_1, x_2, b_1, b_2), \\ f_2(q^2) &= 8\pi C_F m_B^2 \int_0^1 [dx] \int_0^\infty b_1 db_1 b_2 db_2 \phi_B(x_1, b_1) \\ &\quad \times \left\{ \left[ (1 + x_2 \eta) \phi_K(x_2) + 2r_K \left( \frac{1}{\eta} - x_2 \right) \phi_K^t(x_2) - x_2 \phi_K^p(x_2) \right] \right. \\ &\quad \times E(t^{(1)}) h^K(x_1, x_2, b_1, b_2) \\ &\quad \left. + 2r_K \phi_K^p(x_2) E(t^{(2)}) h^K(x_2, x_1, b_2, b_1) \right\}, \end{aligned} \quad (7)$$

and

$$\begin{aligned}
f_T(q^2) &= 8\pi C_F m_B^2 (1 + r_K) \int_0^1 [dx] \int_0^\infty b_1 db_1 b_2 db_2 \phi_B(x_1, b_1) \\
&\times \left\{ [\phi_K(x_2) - r_K x_2 (\phi_K^p(x_2) - \phi_K^t(x_2))] E(t^{(1)}) h^K(x_1, x_2, b_1, b_2) \right. \\
&\left. + 2r_K \phi_K^p(x_2) E(t^{(2)}) h^K(x_2, x_1, b_2, b_1) \right\}. \tag{8}
\end{aligned}$$

From Eq. (6), we find that  $f_+(0) = f_0(0)$ . The evolution factor is given by

$$E(t) = \alpha_s(t) \exp(-S_B(t) - S_K(t)), \tag{9}$$

where the Sudakov exponents  $S_{B(K)}$  are given in Ref. [21]. The hard functions of  $h$  are written as

$$\begin{aligned}
h(x_1, x_2, b_1, b_2) &= S_t(x_2) K_0(\sqrt{x_1 x_2 \eta} m_B b_1) \\
&\times [\theta(b_1 - b_2) K_0(\sqrt{x_2 \eta} m_B b_1) I_0(\sqrt{x_2 \eta} m_B b_2) \\
&+ \theta(b_2 - b_1) K_0(\sqrt{x_2 \eta} m_B b_2) I_0(\sqrt{x_2 \eta} m_B b_1)] \tag{10}
\end{aligned}$$

where the threshold resummation effect is described by [8]

$$S_t(x) = \frac{2^{1+2c} \Gamma(\frac{3}{2} + c)}{\sqrt{\pi} \Gamma(1 + c)} [x(1-x)]^c.$$

The hard scales  $t^{(1,2)}$  are chosen to be

$$\begin{aligned}
t^{(1)} &= \max(\sqrt{m_B^2 \eta x_2}, 1/b_1, 1/b_2), \\
t^{(2)} &= \max(\sqrt{m_B^2 \eta x_1}, 1/b_1, 1/b_2).
\end{aligned}$$

In Ref. [12], we have given detailed discussions and expressions for all form factors in the  $B \rightarrow K^*$  transition based on the PQCD in the large recoil region. We emphasize that in the PQCD approach there is an identity at  $q^2 = 0$ , given by [12]

$$A_2(0) = (1 + r_{K^*})^2 A_1(0) - 2r_{K^*} (1 + r_{K^*}) A_0(0),$$

which is consistent with the leading order model-independent relation [1, 22, 23, 24, 25, 26]

$$A_2(0) = \frac{1 + r_{K^*}}{1 - r_{K^*}} A_1(0) - \frac{2r_{K^*}}{1 - r_{K^*}} A_0(0).$$

Table 1: Form factors for  $B \rightarrow K^*$  in the LEET and PQCD with (I)  $\omega_B = 0.40$  and (II)  $\omega_B = 0.42$ .

	$V(0)$	$A_0(0)$	$A_1(0)$	$A_2(0)$	$T_1(0)$	$T_3(0)$
LEET[24]	$0.36 \pm 0.04$		$0.27 \pm 0.03$		$0.31 \pm 0.02$	
PQCD (I)	0.355	0.407	0.266	0.202	0.315	0.207
(II)	0.332	0.381	0.248	0.189	0.294	0.193

In our numerical calculations, we use  $f_B = 0.19$  GeV,  $f_{K^*} = 0.21$  GeV,  $f_{K^*}^T = 0.17$  GeV,  $m_B = 5.28$  GeV,  $m_{K^*} = 0.892$  GeV, and  $c = 0.3$  (0.4) for  $B \rightarrow K$  ( $K^*$ ), and we take the  $B$  meson wave function as [21, 8]

$$\phi_B(x, b) = N_B x^2 (1-x)^2 \exp \left[ -\frac{1}{2} \left( \frac{xM_B}{\omega_B} \right)^2 - \frac{\omega_B^2 b^2}{2} \right], \quad (11)$$

where  $\omega_B$  is the shape parameter [27] and  $N_B$  is determined by the normalization of the wave function, given by

$$\int_0^1 dx \phi_B(x, 0) = \frac{f_B}{2\sqrt{2N_c}}.$$

Since the shape parameter  $\omega_B$  and chiral symmetry breaking parameter  $m_K^0$  are free in the PQCD, in order to estimate the uncertainties, we choose (I)  $\omega_B = 0.40$  and (II)  $\omega_B = 0.42$  for  $B \rightarrow K^*$  and (I)  $\omega_B = 0.40$  and  $m_K^0 = 1.7$  and (II)  $\omega_B = 0.42$  and  $m_K^0 = 1.5$  for  $B \rightarrow K$  as the upper and lower bounds, respectively. From these values, we obtain the form factors of  $B \rightarrow K$  at  $q^2 = 0$  as: (I)  $f_+ = 0.354$  and  $f_T = 0.250$  and (II)  $f_+ = 0.303$  and  $f_T = 0.220$ , while those for the  $B \rightarrow K^*$  ones are shown in Table 1. It is known that at the small  $q^2$  region there exists a large energy effective theory (LEET) so that all form factors for heavy-to-light decays can be described by few independent functions [23]. In Table 1, we also show the results found by combining the LEET with the experimental data of  $B \rightarrow K^* \gamma$  [24]. We note that our results for the form factors are different from those in Ref. [4], which shall be referred as (III). We remark that we have neglected nonlocal contributions from the four-quark operators. These effects can contribute in the 5 – 10% range to the form factors [28].

Table 2: Form factors in  $B \rightarrow K$  from the HQET and lattice calculations at some large values of  $q^2$ .

$q^2$ GeV <sup>2</sup>	$f_+(q^2)$	$f_0(q^2)$	$f_T(q^2)$
21	$1.61 \pm 0.11$	$0.61 \pm 0.03$	$1.54 \pm 0.12$
22	$2.05 \pm 0.12$	$0.67 \pm 0.03$	$1.99 \pm 0.13$

## 2.2 At zero recoil

### 2.2.1 Form factors in $B \rightarrow K$

According to the analysis of Ref. [19], under the heavy quark symmetry, the form factor of  $f_T(q^2)$  in  $B \rightarrow K$  can be written in terms of two independent form factors as

$$f_T(q^2) = \frac{m_B + m_P}{2m_B}(f_+(q^2) - f_-(q^2)) \quad (12)$$

where  $f_-(q^2) = (m_B^2 - m_K^2)(f_0(q^2) - f_+(q^2))/q^2$ . Since there is no complete lattice calculations on the form factors in  $B \rightarrow K$  in the literature yet, the strategy to obtain  $f_+$  and  $f_-$  is that we utilize the relationships, which connect the form factors between  $B \rightarrow K$  and  $D \rightarrow K$  with the HQET, given by [19]

$$\begin{aligned} f_+^B(v \cdot p) &= \frac{1}{2} \left( \frac{m_B}{m_D} \right)^{1/2} \left( \frac{\alpha_s(m_b)}{\alpha_s(m_c)} \right)^{-(6/25)} \left[ \left( 1 + \frac{m_D}{m_B} \right) f_+^D(v \cdot p) - \left( 1 - \frac{m_D}{m_B} \right) f_-^D(v \cdot p) \right], \\ f_-^B(v \cdot p) &= \frac{1}{2} \left( \frac{m_B}{m_D} \right)^{1/2} \left( \frac{\alpha_s(m_b)}{\alpha_s(m_c)} \right)^{-(6/25)} \left[ \left( 1 + \frac{m_D}{m_B} \right) f_-^D(v \cdot p) - \left( 1 - \frac{m_D}{m_B} \right) f_+^D(v \cdot p) \right], \end{aligned} \quad (13)$$

where  $\left( \alpha_s(m_b)/\alpha_s(m_c) \right)^{-(6/25)}$  is the relevant renormalization factor. We note that the form factors  $f_{+(-)}^B(v \cdot p)$  are evaluated at the same value of  $v \cdot p$  as  $f_{+(-)}^D(v \cdot p)$ . In order to get the values at zero recoil, we adopt the lattice results in  $D \rightarrow K$  [29], where the predicted BR for  $D \rightarrow K \ell \nu$  is consistent with the measurement [30]. From Eqs. (12) and (13), we find the form factors shown in Table 2 in the large  $q^2$  region. In Table 3, we show the form factors in  $B \rightarrow K$  at  $q^2 = 0$  and fitted parameters of  $\sigma_{1,2}$  in Eq. (2).

### 2.2.2 Form factors in $B \rightarrow K^*$

We calculate the form factors in  $B \rightarrow K^*$  by using the same technique as that in  $B \rightarrow K$ . Following the HQET, we have the relations given by [19, 31]

$$T_1(q^2) = \frac{m_B^2 + q^2 - m_V^2}{2m_B} \frac{V(q^2)}{m_B + m_V} + \frac{m_B + m_V}{2m_B} A_1(q^2),$$



Table 3: Form factors in  $B \rightarrow K$  at  $q^2 = 0$  and fitted parameters of  $\sigma_{1,2}$  in Eq. (2).

	$f_+(q^2)$	$f_0(q^2)$	$f_T(q^2)$
(I) $q^2 = 0$	0.354	0.354	0.25
$\sigma_1$	-1.246	-0.297	-1.570
$\sigma_2$	0.251	-0.400	0.584
(II) $q^2 = 0$	0.303	0.303	0.220
$\sigma_1$	-1.229	-1.212	-1.496
$\sigma_2$	0.219	0.755	0.492

$$\begin{aligned}
T_1(q^2) - T_2(q^2) &= \frac{q^2}{m_B^2 - m_V^2} \left[ \frac{3m_B^2 - q^2 + m_V^2}{2m_B} \frac{V(q^2)}{m_B + m_V} - \frac{m_B + m_V}{2m_B} A_1(q^2) \right], \\
T_3(q^2) &= \frac{m_B^2 - q^2 + 3m_V^2}{2m_B} \frac{V(q^2)}{m_B + m_V} + \frac{m_B^2 - m_V^2}{m_B q^2} m_V A_0(q^2), \\
&- \frac{m_B^2 + q^2 - m_V^2}{2m_B q^2} \left[ (m_B + m_V) A_1(q^2) - (m_B - m_V) A_2(q^2) \right]. \quad (14)
\end{aligned}$$

We remark that the above identities are valid only for  $q^2$  close to the zero recoil region where the HQET is reliable. We note that the relations in Eq. (14) are not complete as they mix terms of different order in  $1/m_b$  in the zero recoil region [32]. The correct treatment has been given recently in Ref. [33]. From Eq. (14), we find that  $V(q^2)$ ,  $A_1(q^2)$ , and  $T_3(q^2)$  can be determined once  $T_{1,2}(q^2)$  and  $A_{0,2}(q^2)$  are fixed. In Table 4, we display the form factors in  $B \rightarrow K^*$ , where we have used Eq. (14) in the HQET and the lattice QCD results [20] of  $T_{1,2}(q^2)$  and  $A_{0,2}(q^2)$ , which have been demonstrated to be consistent with the measurement in  $B \rightarrow K^* \gamma$ . We remark that  $A_0(q^2) = T_1(q^2)$  has been taken in the lattice calculations. The form factors in  $B \rightarrow K^*$  at  $q^2 = 0$  and fitted parameters of  $\sigma_{1,2}$  in Eq. (2) are shown in Table 5.

Table 4: Form factors for  $B \rightarrow K^*$  from the lattice results of  $T_{1,2}(q^2)$  and  $A_{0,2}(q^2)$  with the HQET at some values of higher  $q^2$ .

$q^2$ GeV <sup>2</sup>	$V(q^2)$	$A_1(q^2)$	$A_2(q^2)$	$T_1(q^2)$	$T_2(q^2)$	$T_3(q^2)$
16	$1.33 \pm 0.05$	$0.44 \pm 0.02$	$0.67 \pm 0.03$	$1.14 \pm 0.04$	$0.47 \pm 0.02$	$0.67 \pm 0.03$
17	$1.50 \pm 0.05$	$0.46 \pm 0.01$	$0.72 \pm 0.02$	$1.28 \pm 0.04$	$0.48 \pm 0.01$	$0.73 \pm 0.02$
19	$1.94 \pm 0.03$	$0.49 \pm 0.01$	$0.82 \pm 0.01$	$1.66 \pm 0.02$	$0.49 \pm 0.01$	$0.86 \pm 0.01$

Table 5: Form factors in  $B \rightarrow K^*$  at  $q^2 = 0$  and fitted parameters of  $\sigma_{1,2}$  in Eq. (2).

	$V(q^2)$	$A_0(q^2)$	$A_1(q^2)$	$A_2(q^2)$	$T_1(q^2)$	$T_2(q^2)$	$T_3(q^2)$
(I) $q^2 = 0$	0.355	0.407	0.266	0.202	0.315	0.315	0.207
$\sigma_1$	-1.802	-1.282	-1.034	-1.906	-1.749	-0.975	-1.777
$\sigma_2$	0.879	0.249	0.514	1.168	0.816	0.632	0.964
(II) $q^2 = 0$	0.332	0.381	0.248	0.189	0.294	0.294	0.193
$\sigma_1$	-1.721	-1.228	-0.829	-1.801	-1.671	-0.721	-1.677
$\sigma_2$	0.744	0.148	0.166	0.993	0.684	0.202	0.794

### 3 Differential Decay Rates and polarizations

From the definitions of form factors in Eq. (1), in the SM the transition amplitudes for  $B \rightarrow K^{(*)}\ell^+\ell^-$  ( $\ell = e, \mu$ ) can be written as

$$\mathcal{M}_K = \frac{G_F \alpha \lambda_t}{2\sqrt{2}\pi} \left\{ \left[ C_9^{eff}(\mu) f_+(q^2) + 2m_b C_7(\mu) \frac{f_T(q^2)}{m_B + m_K} \right] P_\mu \bar{\ell} \gamma^\mu \ell + C_{10} f_+(q^2) P_\mu \bar{\ell} \gamma^\mu \gamma_5 \ell \right\} \quad (15)$$

and

$$\mathcal{M}_{K^*}^{(\lambda)} = \frac{G_F \alpha \lambda_t}{2\sqrt{2}\pi} \left\{ \mathcal{M}_{1\mu}^{(\lambda)} \bar{\ell} \gamma^\mu \ell + \mathcal{M}_{2\mu}^{(\lambda)} \bar{\ell} \gamma^\mu \gamma_5 \ell \right\} \quad (16)$$

with

$$\mathcal{M}_{i\mu}^{(\lambda)} = i\xi_1 \varepsilon_{\mu\nu\alpha\beta} \epsilon^{*\nu}(\lambda) P^\alpha q^\beta + \xi_2 \epsilon_\mu^*(\lambda) + \xi_3 \epsilon^* \cdot q P_\mu, \quad (17)$$

where we have set  $m_\ell = 0$  ( $\ell = e, \mu$ ),  $\lambda_t = V_{tb} V_{ts}^* \simeq 0.041 \pm 0.002$  [34],  $C_i^{(eff)}$  are the Wilson coefficients (WCs) and their expressions can be found in Refs. [4, 35], and  $i = 1$  (2) for  $\xi_j = h_j$  ( $g_j$ ) with  $j = 1, 2, 3$ , defined in Appendix.

For the decays of  $B \rightarrow K\ell^+\ell^-$ , since the  $K$  meson is a pseudo-scalar, the only interesting physical observables are the decay rates themselves, whereas other observables such as the lepton polarizations, discussed in detail in Refs. [1, 2, 3, 4], are hard to be measured by experiments. The differential decay rates for  $B \rightarrow K\ell^+\ell^-$  are given by [4]

$$\frac{d\Gamma_K(s)}{ds} = \frac{G_F^2 \alpha^2 |\lambda_t|^2 m_B^5}{3 \times 2^9 \pi^5} (1-s)^{3/2} \left[ \left| C_9^{eff}(\mu) f_+(q^2) + 2m_b C_7(\mu) f_T(q^2) \right|^2 + \left| C_{10} f_+(q^2) \right|^2 \right] \quad (18)$$

where  $s = q^2/M_B^2$ . For  $B \rightarrow K^*\ell^+\ell^-$ , however, one can study not only the decay rates and lepton polarizations but also physical observables related to the  $K^*$  polarization, including longitudinal and transverse polarizations of  $K^*$  and P and T-odd observables. To analyze the polarization of  $K^*$ , we have to consider the decay chain  $B \rightarrow K^*\ell^+\ell^- \rightarrow K\pi\ell^+\ell^-$ , and

we choose the  $K^*$  helicities as  $\epsilon(0) = (|\vec{p}_{K^*}|, 0, 0, E_{K^*})/M_{K^*}$  and  $\epsilon(\pm) = (0, 1, \pm i, 0)/\sqrt{2}$ , the positron lepton momentum  $p_{l^+} = \sqrt{q^2}(1, \sin \theta_l, 0, \cos \theta_l)/2$  with  $E_{K^*} = (M_B^2 - M_{K^*}^2 - q^2)/2\sqrt{q^2}$  and  $|\vec{p}_{K^*}| = \sqrt{E_{K^*}^2 - M_{K^*}^2}$  in the  $q^2$  rest frame, and the  $K$  momentum  $p_K = (1, \sin \theta_K \cos \phi, \sin \theta_K \sin \phi, \cos \theta_K)M_{K^*}/2$  in the  $K^*$  rest frame where  $\phi$  denotes the relative angle of decaying plane between  $K\pi$  and  $l^+l^-$ . From Eq. (16), the differential decay rates of  $B \rightarrow K^*\ell^+\ell^- \rightarrow K\pi\ell^+\ell^-$  as functions of angles  $\theta_K$  and  $\phi$  are found to be

$$\begin{aligned} \frac{d\Gamma}{d\cos\theta_K d\phi dq^2} &= \frac{G_F^2 \alpha^2 |\lambda_t|^2 |\vec{p}|}{2^{14} \pi^6 m_B^2} Br(K^* \rightarrow K\pi) \\ &\times \left\{ 16 \cos^2 \theta_K \sum_{i=1,2} |\mathcal{M}_i^0|^2 \right. \\ &+ 8 \sin^2 \theta_K \sum_{i=1,2} (|\mathcal{M}_i^+|^2 + |\mathcal{M}_i^-|^2) \\ &- 8 \sin^2 \theta_K \left[ \cos 2\phi \sum_{i=1,2} Re \mathcal{M}_i^+ \mathcal{M}_i^{-*} + \sin 2\phi \sum_{i=1,2} Im \mathcal{M}_i^+ \mathcal{M}_i^{-*} \right] \\ &+ 3\pi \sin 2\theta_K \left[ \cos \phi (Re \mathcal{M}_1^0 (\mathcal{M}_2^{+*} - \mathcal{M}_2^{-*}) + Re (\mathcal{M}_1^+ - \mathcal{M}_1^-) \mathcal{M}_2^{0*}) \right. \\ &\left. + \sin \phi (Im \mathcal{M}_1^0 (\mathcal{M}_2^{+*} + \mathcal{M}_2^{-*}) - Im (\mathcal{M}_1^+ + \mathcal{M}_1^-) \mathcal{M}_2^{0*}) \right] \left. \right\} \end{aligned} \quad (19)$$

with

$$\begin{aligned} |\vec{p}| &= \sqrt{E'^2 - m_{K^*}^2}, \quad E' = \frac{m_B^2 + m_{K^*}^2 - q^2}{2m_B}, \\ \mathcal{M}_a^0 &= \sqrt{q^2} \left( \frac{E_{K^*}}{m_{K^*}} \xi_2 + 2\sqrt{q^2} \frac{|p_{K^*}|^2}{m_{K^*}} \xi_3 \right), \\ \mathcal{M}_a^\pm &= \sqrt{q^2} (\pm 2|p_{K^*}| \sqrt{q^2} \xi_1 + \xi_2), \end{aligned} \quad (20)$$

where  $a = 1(2)$ . We note that other discussions for various polarizations can be in Refs. [36, 37, 38]. From Eq. (19), by integrating all angles we obtain

$$\frac{d\Gamma_{K^*}(s)}{ds} = \frac{G_F^2 \alpha^2 |\lambda_t|^2 |\vec{p}|}{3 \times 2^8 \pi^5} \sum_{\lambda=+,0,-} \sum_{i=1,2} |\mathcal{M}_i^\lambda|^2, \quad (21)$$

where we have used that  $Br(K^* \rightarrow K\pi) = 1$  [30].

The components  $\mathcal{M}_a^0$  and  $\mathcal{M}_a^\pm$  in Eq. (20) clearly denote the longitudinal and transverse polarizations, which can be extracted by integrating out the angle  $\phi$  dependence in Eq. (19), respectively, and explicitly we have that

$$\begin{aligned} \frac{d\Gamma}{dq^2 d\cos\theta_K} &= \frac{G_F^2 \alpha^2 |\lambda_t|^2 |\vec{p}|}{2^{10} \pi^5 m_B^2} Br(K^* \rightarrow K\pi) \left\{ 2 \cos^2 \theta_K \sum_{i=1,2} |\mathcal{M}_i^0|^2 \right. \\ &\left. + \sin^2 \theta_K \sum_{i=1,2} (|\mathcal{M}_i^+|^2 + |\mathcal{M}_i^-|^2) \right\}, \end{aligned} \quad (22)$$

From Eqs. (21) and (22), we may define

$$\mathcal{P}_L(q^2) = \frac{\sum_{i=1,2} |\mathcal{M}_i^0|^2}{\sum_{\lambda=+,0,-} \sum_{i=1,2} |\mathcal{M}_i^\lambda|^2}, \quad (23)$$

$$\mathcal{P}_T(q^2) = \frac{\sum_{i=1,2} (|\mathcal{M}_i^+|^2 + |\mathcal{M}_i^-|^2)}{\sum_{\lambda=+,0,-} \sum_i |\mathcal{M}_i^\lambda|^2}, \quad (24)$$

as the normalized longitudinal and transverse parts with their ratio being

$$\xi(q^2) = \frac{\mathcal{P}_T(q^2)}{\mathcal{P}_L(q^2)} = \frac{\sum_{i=1,2} (|\mathcal{M}_i^+|^2 + |\mathcal{M}_i^-|^2)}{\sum_{i=1,2} |\mathcal{M}_i^0|^2}. \quad (25)$$

In Figures 1 and 2, we show the differential decay rates of  $B \rightarrow K^{(*)}\mu^+\mu^-$  as functions of  $s = q^2/M_B^2$  with and without resonant  $\bar{c}c$  states, respectively. From both figures, it is obvious to see that the dilepton invariant distributions for the two modes are quite different. However, we expect that the distribution for  $B \rightarrow K\ell^+\ell^-$ , which contains only the longitudinal part due to the angular momentum conservation, is similar to the corresponding part in  $B \rightarrow K^*\ell^+\ell^-$ . For  $B \rightarrow K^*\ell^+\ell^-$ , the transverse part, associated with  $1/q^2$  from the  $\gamma$ -penguin diagram described by  $C_7(\mu)$ , gives the dominant contribution when  $q^2$  goes to the allowed minimal values of  $4m_\ell^2$ . This not only explains why the differential decay rates increase as  $q^2 \rightarrow 0$  but also indicates the reason for the difference between BRs in  $B \rightarrow K^*e^+e^-$  and  $B \rightarrow K^*\mu^+\mu^-$ .

Using Eq. (21) and the fitted form factors in Tables 5 and 3, we obtain

$$\begin{aligned} Br(B \rightarrow K\ell^+\ell^-) &= (0.53 \pm 0.05_{-0.07}^{+0.10}) \times 10^{-6}, \\ Br(B \rightarrow K^*e^+e^-) &= (1.68 \pm 0.17_{-0.09}^{+0.14}) \times 10^{-6}, \\ Br(B \rightarrow K^*\mu^+\mu^-) &= (1.34 \pm 0.13_{-0.06}^{+0.11}) \times 10^{-6}, \end{aligned} \quad (26)$$

where the first and second errors are from  $\lambda_\ell$  and the hadronic effects, shown in Tables 3 and 5, respectively. We remark that the central value of Eq. (26) for  $B \rightarrow K^*e^+e^-$  is the same as the BABAR recent measured value [7] and it is much smaller than that in (III) of Ref. [4] but that for  $B \rightarrow K^*\mu^+\mu^-$  a little larger.

In Figure 3, we present the effects of  $K^*$  longitudinal and transverse polarizations based on Eqs. (23) and (24). In Figure 4, we display the ratio of  $\xi(q^2)$  and we see that when  $s \leq 0.016$ , where  $B \rightarrow K^*\gamma$  is the main effect, and  $s \geq 0.339$ , where the longitudinal contribution is suppressed, the transverse part of the  $K^*$  polarization becomes dominant. We find that both  $\mathcal{P}_L$  and  $\mathcal{P}_T$  as well as  $\xi(q^2)$  are insensitive to the hadronic uncertainties in (I) and (II). Moreover, the differences between the results of (I,II) and (III) are small.

## 4 T and P violating effects

The terms with imaginary parts in Eq. (19) are related to *T odd* effects which, without final state interactions, are *T violating* and thus *CP violating* due to the CPT theorem. In a three-body decay, the triple correlations such as  $\vec{s}_k \cdot \vec{p}_i \times \vec{p}_j$  are examples of the effects, where  $\vec{s}_k$  denotes the spin vector carried by one of involving particles and  $\vec{p}_{i,j}$  are the momentum vectors of outgoing particles. In the decays of  $B \rightarrow K^* \ell^+ \ell^-$ , the spin  $s_k$  can be either the polarized lepton,  $s_\ell$ , or the  $K^*$  meson,  $\epsilon^*(\lambda)$ . However, since the lepton polarization is always associated with the lepton mass and expected to be suppressed and less than 1% for the  $e$  or  $\mu$  mode. On the other hand, the T odd effects with  $K^*$  are free of the mass suppression and they can be large in models with new physics [12, 39]. To study these effects, we define [12, 39]

$$\langle \mathcal{O}_i \rangle = \int \mathcal{O}_i \omega_i(u_{\theta_K}, u_{\theta_{\ell^+}}) \frac{d\Gamma}{dq^2} \quad (27)$$

where  $\omega_i(u_{\theta_K}, u_{\theta_{\ell^+}}) = u_{\theta_K} u_{\theta_{\ell^+}} / |u_{\theta_K} u_{\theta_{\ell^+}}|$  are sign functions with  $u_{\theta_i}$  being  $\cos \theta_i$  or  $\sin \theta_i$ . In the  $K^*$  rest frame, we use the T odd momentum correlations as the operators in Eq. (27), given by

$$\mathcal{O}_{T_1} = |\vec{p}_B| \frac{(\vec{p}_B \cdot \vec{p}_{l^+} \times \vec{p}_K)(\vec{p}_B \times \vec{p}_K) \cdot (\vec{p}_{l^+} \times \vec{p}_B)}{|\vec{p}_B \times \vec{p}_K|^2 |\vec{p}_{l^+} \times \vec{p}_B|^2} = \frac{1}{2} \sin 2\phi, \quad (28)$$

$$\mathcal{O}_{T_2} = |\vec{p}_B| \frac{\vec{p}_K \cdot (\vec{p}_B \times \vec{p}_{l^+})}{|\vec{p}_B \times \vec{p}_K| |\vec{p}_B \times \vec{p}_{l^+}|} = \sin \phi, \quad (29)$$

accompanied with sign functions of  $\omega_{T_1}(\sin \theta_K, \sin \theta_{\ell^+})$  and  $\omega_{T_2}(\cos \theta_K, \sin \theta_{\ell^+})$ , respectively. By defining the physical observables as

$$\mathcal{A}_i = \frac{\langle \mathcal{O}_i \rangle}{d\Gamma/dq^2}, \quad (30)$$

from Eqs. (27), (28) and (29) we obtain that

$$\mathcal{A}_{T_1} = -\frac{\sum_{i=1,2} \text{Im}(\mathcal{M}_i^+ \mathcal{M}_i^{-*})}{4 \sum_{\lambda=+,0,-} \sum_{i=1,2} |\mathcal{M}_i^\lambda|^2} \quad (31)$$

$$\mathcal{A}_{T_2} = \frac{3\pi \text{Im} \mathcal{M}_1^0 (\mathcal{M}_2^{+*} + \mathcal{M}_2^{-*}) - \text{Im}(\mathcal{M}_1^+ + \mathcal{M}_1^-) \mathcal{M}_2^{0*}}{16 \sum_{\lambda=+,0,-} \sum_{i=1,2} |\mathcal{M}_i^\lambda|^2} \quad (32)$$

We note that as shown in Refs. [12, 39]  $\mathcal{A}_{T_1}$  and  $\mathcal{A}_{T_2}$  depend on  $\text{Im} C_9^{eff}(\mu) C_7(\mu)^*$  and  $\text{Im} C_7(\mu) C_{10}^*$ , respectively. In the SM,  $\mathcal{A}_{T_2}$  is zero since there are no absorptive parts expected

from  $C_7$  and  $C_{10}$ , whereas  $\mathcal{A}_{T_1}$  is non-zero due to that from  $C_9^{eff}$ . However, it is clear that the T-odd observable of  $\mathcal{A}_{T_2}$  can be large in models with new CP violating phases beyond the SM. To illustrate a new physics result, in Figure 5 we show the T violating effect of  $\mathcal{A}_{T_2}$  as a function of  $s$  by taking two cases with the imaginary parts of WCs as follows: (i)  $ImC_7(\mu) = 0.25$  and (ii)  $ImC_7(\mu) = 0.25$  and  $ImC_{10} = -2.0$ . One possible origin of having these imaginary parts is from SUSY [39] where there are many CP violating sources. Here, we only show the cases with (I) and (III) while those in (II) are almost the same as (I). It is interesting to note that the CP violating effect can be as large as 15% in both cases as shown in Figure 5. We remark that  $\mathcal{A}_{T_1}$  is much smaller than  $\mathcal{A}_{T_2}$  in most of cases with new physics.

From Eq. (19), we can also study another interesting physical observable associated with the angular distribution of  $\sin 2\theta_K \cos \phi$  in  $B \rightarrow K^* \ell^+ \ell^- \rightarrow K \pi \ell^+ \ell^-$ . This observable is defined as an up-down asymmetry (UDA) of the  $K$  meson due to its dependence of  $\cos \theta_K$ . Explicitly, we define that

$$\begin{aligned} \mathcal{O}_{UD} &= \frac{(\vec{p}_B \times \vec{p}_K) \cdot (\vec{p}_{\ell^+} \times \vec{p}_B)}{|\vec{p}_B \times \vec{p}_K| |\vec{p}_{\ell^+} \times \vec{p}_B|} = \cos \phi, \\ \omega(u_{\theta_K}, u_{\theta_\ell}) &= \omega(\cos \theta_K, \sin \theta_\ell), \end{aligned} \quad (33)$$

as the operator corresponding to the UDA of  $K$  in the  $K^*$  ( $\rightarrow K\pi$ ) rest frame and from Eqs. (19), (27) and (30) we find that

$$\mathcal{A}_{UD}^K(q^2) \equiv \frac{\langle \mathcal{O}_{UD} \rangle}{d\Gamma/dq^2} = \frac{3\pi \operatorname{Re} \mathcal{M}_1^0 (\mathcal{M}_2^{+*} - \mathcal{M}_2^{-*}) + \operatorname{Re} (\mathcal{M}_1^+ - \mathcal{M}_1^-) \mathcal{M}_2^{0*}}{16 \sum_{\lambda=+,0,-} \sum_{i=1,2} |\mathcal{M}_i^\lambda|^2}, \quad (34)$$

which clearly violates parity.

In Figure 6a, we show the  $\mathcal{A}_{UD}^K(s)$  as a function of  $s = q^2/M_B^2$  based on the form factors given by the PQCD (I), (II) and (III) in the SM. It is interesting to point out that, as shown in the figure, in the SM  $\mathcal{A}_{UD}^K(s)$  crosses zero point at  $s_0 \simeq 0.08$  which satisfies the identity

$$\operatorname{Re}(h_1 g_2^* + h_2 g_1^*) = -2 \frac{\sqrt{m_B^2 s_0} |\vec{p}_{K^*}|^2}{E_{K^*}} \operatorname{Re}(h_3 g_1^* + h_1 g_3^*). \quad (35)$$

We note that the point  $s_0$  is insensitive the QCD models but the Wilson coefficients of  $C_7(\mu)$  and  $C_9(\mu)$ , especially the relative sign between them. To show the result, in Figure 6b we present two extreme cases of (i)  $C_7(\mu) = -C_7(\mu)_{SM}$  (solid curve) and (ii)  $C_9(\mu) = -C_9(\mu)_{SM}$  (dash-dotted curve) with the remaining Wilson coefficients the same as those in the SM, respectively. From the figure, we see that the distributions in the two cases are quite different

and moreover,  $s_0$  disappears, *i.e.*, it exists only if  $C_7(\mu)$  and  $C_9(\mu)$  have an opposite sign since  $C_7(\mu)_{SM} < 0$  and  $C_9(\mu)_{SM} > 0$ . It is clear that  $s_0$  provides us a good candidate to explore new physics due to the insensitivity of the QCD models and dependence on the WCs.

## 5 Conclusions

We have studied the exclusive decays of  $B \rightarrow K^{(*)}\ell^+\ell^-$  by the results in the PQCD with the HQET and LQCD. We have given the form factors for the  $B \rightarrow K^{(*)}$  transitions in the whole allowed region, which are consistent with those from other QCD models. We have found that the branching ratios of  $B \rightarrow K\ell^+\ell^-$ ,  $B \rightarrow K^*e^+e^-$ , and  $B \rightarrow K^*\mu^+\mu^-$  are  $0.53 \pm 0.05_{-0.07}^{+0.10}$ ,  $1.68 \pm 0.17_{-0.09}^{+0.14}$ , and  $1.34 \pm 0.13_{-0.06}^{+0.11} \times 10^{-6}$ , respectively. We have shown that, in  $B \rightarrow K^*\ell^+\ell^- \rightarrow K\pi\ell^+\ell^-$ , the T-odd observable of  $\mathcal{A}_{T2}$  which is unmeasurably small in the SM could be as large as 20% in models with new physics, while the P-odd up-down asymmetry of  $\mathcal{A}_{UD}^K(s)$  vanishes at  $s_0 \simeq 0.08$  in the SM but it behaves quite differently if new physics exists, which provide us unique probes of non-standard physics.

## Acknowledgments

This work was supported in part by the National Science Council of the Republic of China under Contract Nos. NSC-90-2112-M-001-069 and NSC-90-2112-M-007-040 and the National Center for Theoretical Science.

## Appendix

The parameters of  $h_{1,2,3}$  and  $g_{1,2,3}$  in Eq. (17) are defined by

$$\begin{aligned}
 h_1 &= C_9(\mu) \frac{V(q^2)}{m_B + m_{K^*}} + \frac{2m_b}{q^2}(\mu) C_7(\mu) T_1(q^2), \\
 h_2 &= -C_9(\mu)(m_B + m_{K^*}) A_1(q^2) - \frac{2m_b}{q^2} P \cdot q C_7(\mu) T_2(q^2), \\
 h_3 &= C_9(\mu) \frac{A_2(q^2)}{m_B + m_{K^*}} + \frac{2m_b}{q^2} C_7(\mu) (T_2(q^2) + \frac{q^2}{P \cdot q} T_3(q^2)), \\
 g_1 &= C_{10} \frac{V(q^2)}{m_B + m_{K^*}}, \\
 g_2 &= -C_{10}(m_B + m_{K^*}) A_1(q^2), \\
 g_3 &= C_{10} \frac{A_2(q^2)}{m_B + m_{K^*}}.
 \end{aligned}$$

## References

- [1] A. Ali et. al., *Phys. Rev.* **D61**, 074024 (2000).
- [2] C.Q. Geng and C.P. Kao, *Phys. Rev.* **D57**, 4479 (1998).
- [3] D. Melikhov, N. Nikitin, and S. Simula, *Phys. Rev.* **D57**, 6814 (1998).
- [4] C.H. Chen and C.Q. Geng, *Phys. Rev.* **D63**, 114025 (2001).
- [5] Belle Collaboration, K. Abe et. al., *Phys. Rev. Lett.* **88**, 021801 (2002).
- [6] BABAR Collaboration, B. Aubert *et al.*, *Phys. Rev. Lett.* **88**, 241801 (2002).
- [7] BABAR Collaboration, B. Aubert *et al.*, arXiv:hep-ex/0207082.
- [8] T. Kurimoto, H.N. Li, A.I. Sanda *Phys. Rev.* **D65** 014007 (2002).
- [9] P. Ball, *JHEP* 9809, 005 (1998); P. Ball *et. al.*, *Nucl. Phys.* **B529**, 323 (1998).
- [10] G.P. Lepage and S.J. Brodsky, *Phys. Lett.* **B87**, 359 (1979); *Phys. Rev.* **D22**, 2157 (1980).
- [11] H.N. Li, *Phys. Rev.* **D64**, 014019 (2001); H.N. Li, hep-ph/0102013.
- [12] C.H. Chen and C.Q. Geng, *Nucl. Phys.* **B636**, 338 (2002), arXiv:hep-ph/0203003.
- [13] Y.Y. Keum, H.N. Li, and A.I. Sanda, *Phys. Lett.* **B504**, 6 (2001); *Phys. Rev.* **D63**, 054008 (2001).
- [14] C.D. Lü, K. Ukai, and M.Z. Yang, *Phys. Rev.* **D63**, 074009 (2001).



- [15] C.H. Chen and H.N. Li, Phys. Rev. **D63**, 014003 (2001).
- [16] B. Melic, Phys. Rev. **D59**, 074005 (1999).
- [17] C.H. Chen, Y.Y. Keum and H.N. Li, Phys. Rev. **D64**, 112002 (2001).
- [18] C.H. Chen, Phys. Lett. **B525**, 56 (2002).
- [19] N. Isgur and M. B. Wise, Phys. Rev. **D42**, 2388 (1990).
- [20] UKQCD Collaboration, Phys. Lett. **B416**, 392 (1998).
- [21] C.H. Chen and H.N. Li, Phys. Rev. **D63** 014003 (2001).
- [22] M. Beneke and T. Feldmann, Nucl. Phys. **B592**, 3 (2000).
- [23] J. Charles *et al.*, Phys. Rev. **D60**, 014001 (1999).
- [24] G. Burdman and G. Hiller, Phys. Rev. **D63**, 113008 (2001); G. Burdman, arXiv:hep-ph/0112063.
- [25] D. Melikhov and B. Stech, Phys. Rev. **D62**, 014006 (2000).
- [26] H. Y. Cheng *et. al.*, Phys. Rev. **D55**, 1559 (1997); C.Q. Geng, C.W. Hwang, C.C. Lih, W.M. Zhang, Phys. Rev. **D64**, 114024 (2001).
- [27] M. Bauer and M. Wirbel, Z. Phys. C **42**, 671 (1998).
- [28] M. Beneke, T. Feldmann and D. Seidel, Nucl. Phys. B **612**, 25 (2001).
- [29] A. Abada *et al.*, Nucl. Phys. **B619** 565 (2001).
- [30] D.E. Groom, *et al.* (Particle Data Group), Eur. Phys. J. **C 15**, 1 (2000).
- [31] G. Burdman and J. F. Donoghue, Phys. Lett. **B270**, 55 (1991).
- [32] P. Ball and V. M. Braun, Phys. Rev. D **58**, 094016 (1998).
- [33] B. Grinstein and D. Pirjol, Phys. Lett. B **533**, 8 (2002).
- [34] A.J. Buras, hep-ph/0109197; M. Ciuchini *et al.*, JHEP **0107**, 013 (2001), arXiv:hep-ph/0012308.
- [35] G. Buchalla, A. J. Buras and M. E. Lautenbacher, Rev. Mod. Phys **68**, 1230 (1996).
- [36] C.S. Kim *et. al.*, Phys. Rev. **D62**, 034013 (2000); C. S. Kim, Y. G. Kim and C. D. Lü, *ibid.* **D 64**, 094014 (2001); T. M. Aliev *et. al.*, Phys. Lett. **B511**, 49 (2001); Q. S. Yan *et. al.*, Phys. Rev. D **62**, 094023 (2000).

- [37] F. Kruger *et. al.*, Phys. Rev. D **61**, 114028 (2000) [Erratum-ibid. D **63**, 019901 (2000)].
- [38] Y. Grossman and D. Pirjol, JHEP **0006**, 029 (2000).
- [39] C.H. Chen and C.Q. Geng, Phys. Rev. D **66**, 014007 (2002), arXiv:hep-ph/0205306.

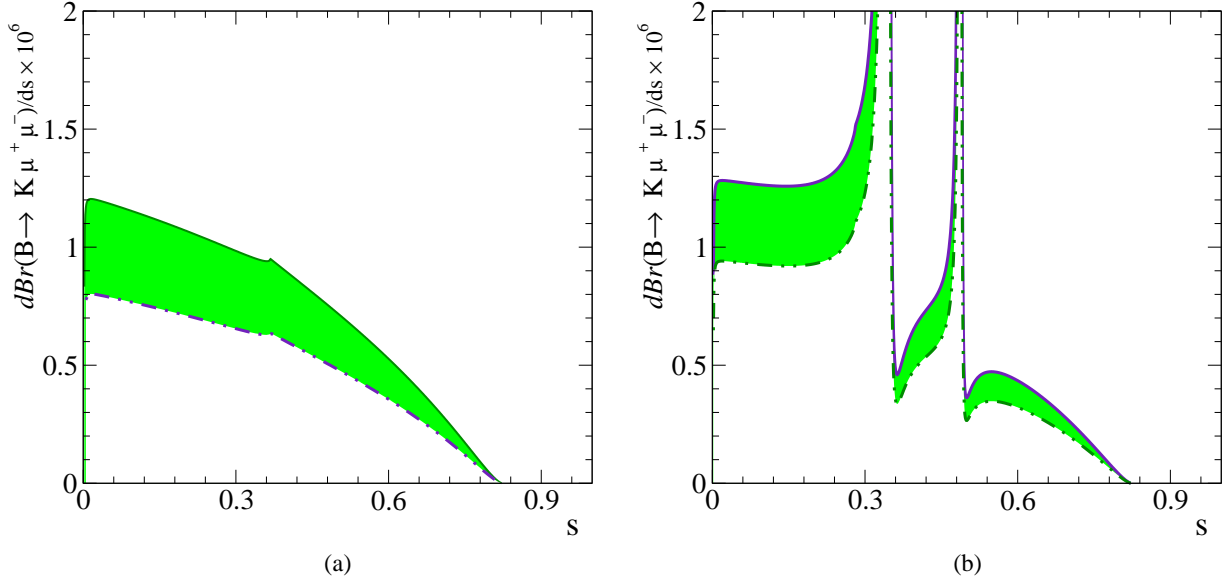


Figure 1: Differential decay BR of  $B \rightarrow K \mu^+ \mu^-$  with (a) and (b) representing the results with and without resonant effect, respectively. The solid (dash-dotted) curve stands for the upper (lower) bound with the allowed region being shaded.

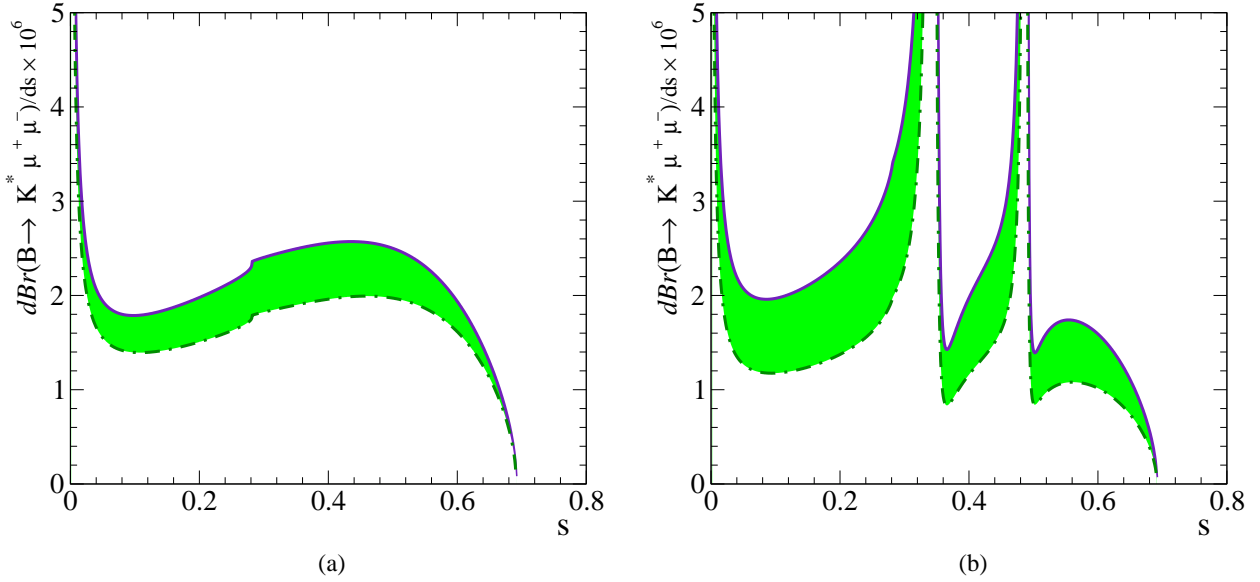


Figure 2: Same as Figure 1 but  $B \rightarrow K^* \mu^+ \mu^+$ .

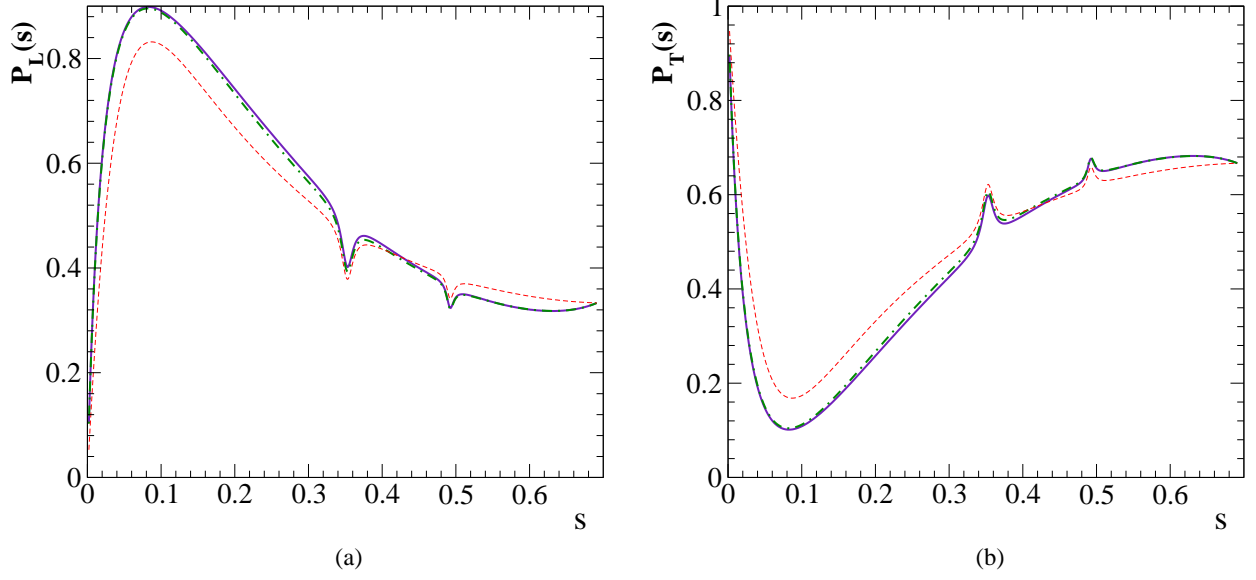


Figure 3: Normalized Longitudinal (a) and transverse (b) polarizations in  $B \rightarrow K^* \mu^+ \mu^-$ . The solid, dash-dotted and dashed curves denote the results from the PQCD (I), (II) and (III) respectively.

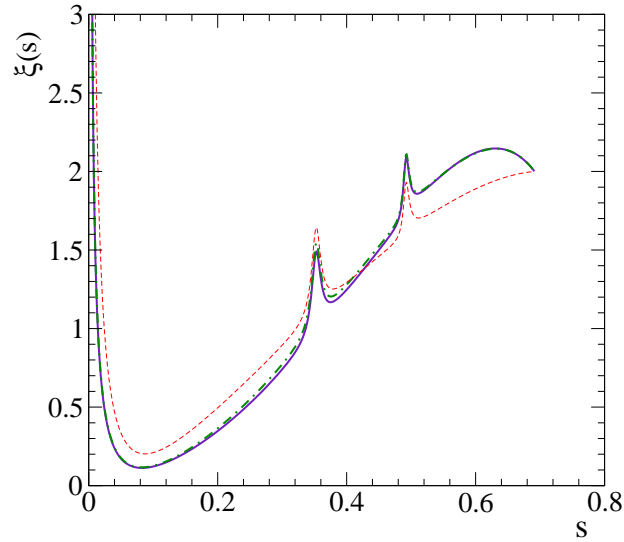


Figure 4: The ratio of  $\xi(s) = \mathcal{P}_T(s)/\mathcal{P}_L(s)$  as a function of  $s$ . Legend is the same as Figure 3.

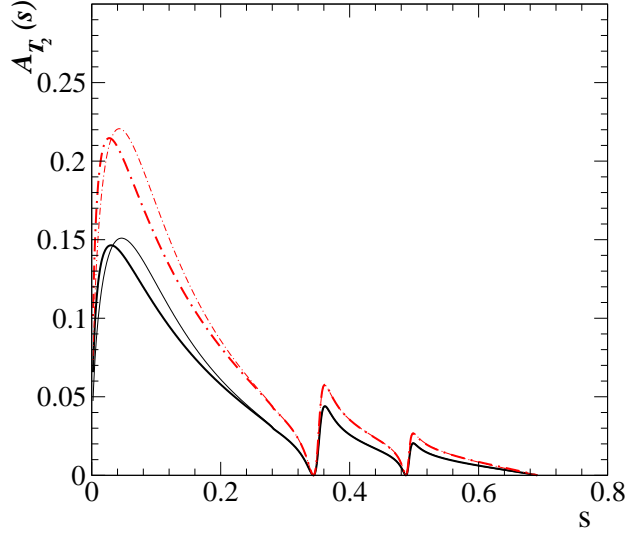


Figure 5:  $T$  violating effect of  $\mathcal{A}_{T_2}(s)$  for (i)  $ImC_7(\mu) = 0.25$  (solid curves) and (ii)  $ImC_7(\mu) = 0.25$  and  $ImC_{10} = -2.0$  (dash-dotted curves), where the bold and thin lines correspond to the PQCD (I) and (III), respectively.

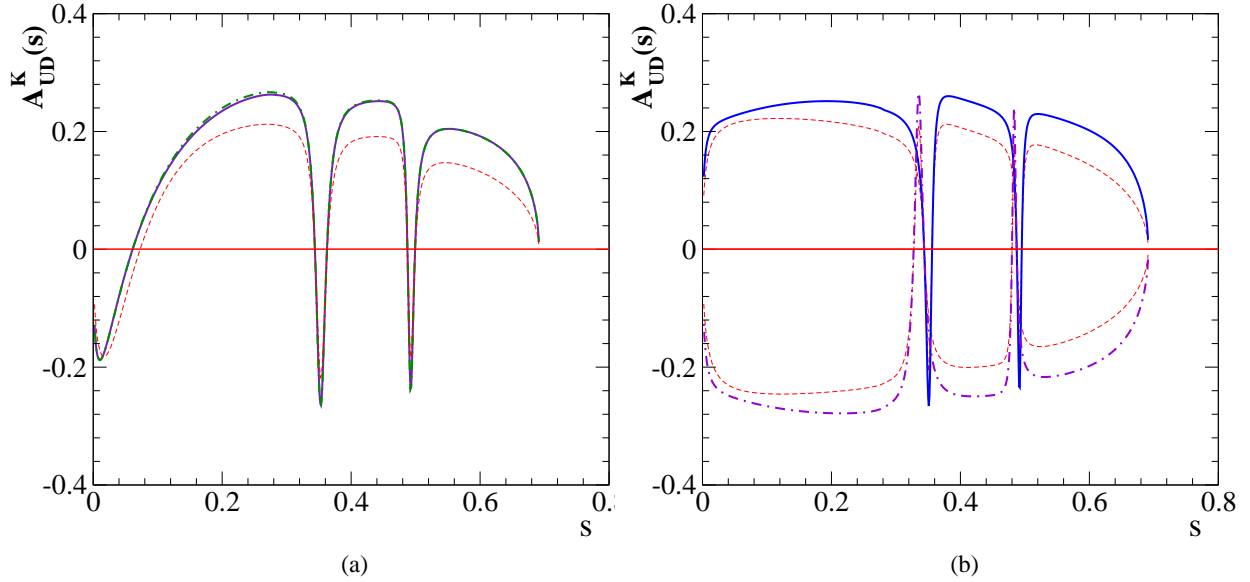


Figure 6:  $\mathcal{A}_{UD}^K(s)$  as a function of  $s$ . In (a) the solid, dash-dotted and dashed curves represent the SM contributions based on the form factors in the PQCD (I), (II) and (III), while in (b) the solid (dash-dotted) and upper (lower) dashed curves are for  $C_7(\mu) > 0$  ( $C_9(\mu) < 0$ ) in (I) and (III), respectively.